OPTIMIZING PHOTOELECTRIC PROPERTIES AND KERR CONSTANTS OF VERTICALLYALIGNED FERROELECTRIC LIQUID CRYSTAL CELLS FOR ADVANCED VEHICLE DISPLAY SYSTEMS

Le Minh Phung[1*]

[1]Dong Nai Technology University

*Corresponding author: Le Minh Phung leminhphung@dntu.edu.vn

GENERAL INFORMATION

Received date: 17/4/2025

Revised date: 29/4/2025

Accepted date: 23/6/2025

KEYWORD

Augmented Reality;

Automotive Applications;

Transparent Displays.

ABSTRACT

This study investigates the photoelectric properties and Kerr constants of vertically-aligned ferroelectric liquid crystal (FLC) cells driven by horizontal electric fields, focusing on applications in vehicle display systems. The research examines the effects of electrode configurations, specifically varying electrode widths (w) and spacing (s), on birefringence and modulation performance. FLC cells were fabricated with three configurations: w = 4 μm, s = 8 μm (Sample A), w = 4 μm, s = 24 μm (Sample B), and w = 8 μm, s = 12 μm (Sample C). Experimental methods included polarized optical microscopy and transmittance-voltage (T-V) measurements, revealing that narrower electrode spacing generated stronger electric fields and faster transmittance changes but were more susceptible to defect formation at higher voltages. Kerr constants were calculated from the T-V data, with Sample B exhibiting the highest Kerr constant (K = 0.769 nm/V²), highlighting its superior modulation capabilities. These findings demonstrate the trade-offs between electrode spacing, electric field strength, and defect stability. The optimized performance of FLC cells offers significant potential for advanced vehicle display applications, including heads-up displays (HUDs) and augmented reality (AR) interfaces, which require high clarity, rapid response, and durability under dynamic driving conditions. This study provides a framework for developing next-generation optical systems tailored to the automotive environment.

1. INTRODUCTION

Ferroelectric liquid crystals (FLCs) have emerged as a promising material for advanced optical and display technologies due to their fast response times and precise phase modulation capabilities under applied electric fields (Yuan et al. 2022). These unique properties position FLCs as ideal candidates for applications in the automotive industry, where high-performance, reliable, and energy-efficient display systems are increasingly in demand (Zhang et al. 2023).

In modern vehicles, the integration of advanced displays for heads-up displays (HUDs), augmented reality (AR) interfaces, and dynamic lighting systems is becoming a standard feature. However, traditional liquid crystal displays face limitations such as slower response times and alignment defects, which impact their performance under dynamic driving conditions (Nájar et al. 2023). The conventional approach of driving deformed-helix ferroelectric liquid crystals (DHFLCs) using vertical electric fields often leads to alignment issues, reducing their effectiveness for automotive use (Nakajima et al. 2024).

Recent advancements suggest that employing horizontally driven electric fields in vertically-aligned DHFLC cells can mitigate alignment defects, enhance birefringence, and improve overall performance (Tkachenko et al. 2024). By optimizing the alignment and electrode configuration, these FLC cells can achieve the high transmittance, rapid modulation, and durability required for automotive display systems (Wyatt et al. 2021).

However, conventional vertically-aligned DHFLC systems are typically driven by vertical electric fields, which often result in defect formation and inconsistent optical responses, making them less suitable for automotive applications. Previous studies have explored electrode patterning and driving schemes, but limited work has focused on the impact of horizontal electric fields on vertically-aligned FLCs with varying electrode geometries. This study addresses this gap by investigating the influence of electrode width and spacing on birefringence and Kerr constants under horizontal driving conditions. Unlike prior methods, this approach offers a promising pathway for improving modulation performance and reducing defect risks in automotive display systems.

This study investigates the photoelectric properties of vertically-aligned DHFLC cells with varying electrode designs to understand their potential for automotive applications (Song et al. 2024). By analyzing the relationship between electrode spacing, birefringence, and Kerr constants, we aim to provide a framework for optimizing FLC-based systems for HUDs, AR displays, and other advanced automotive technologies. The results contribute to the development of next-generation optical systems that meet the rigorous demands of automotive environments.

2. RELATED WORK

The application of liquid crystal technology in the automotive sector has seen significant advancements in recent years (Ali et al. 2022). Liquid crystal displays (LCDs) are widely used in modern vehicles for infotainment systems, instrument clusters, and heads-up displays (HUDs). However, traditional nematic liquid crystals have inherent limitations, such as slower response times and restricted phase modulation capabilities. These challenges impact their ability to meet the demands of real-time information display in dynamic automotive environments (Priscilla et al. 2023).

Ferroelectric liquid crystals (FLCs) have emerged as a promising alternative, offering spontaneous polarization and fast response times. These properties make FLCs ideal for high-speed optical modulation required in advanced display systems (Singh et al. 2021). Research has demonstrated their potential in achieving rapid phase and transmittance changes, aligning well with the automotive industry's demand for high-performance displays, particularly in HUDs and augmented reality (AR) interfaces (Maldonado et al. 2023).

Conventional approaches to driving deformed-helix ferroelectric liquid crystals (DHFLCs) using vertical electric fields often lead to alignment defects, which result in uneven birefringence and compromised optical clarity (Sadigh, Zakerhamidi, and Ranjkesh 2022). This poses significant challenges for applications requiring precision and consistency, such as HUDs. To address these issues, studies have shifted toward alternative alignment techniques and electrode designs that enhance performance while minimizing defects (Khan et al. 2022).

One promising approach involves using horizontal electric fields to drive vertically-aligned FLC cells. This method has been shown to reduce alignment defects and improve optical properties, including increased Kerr constants and enhanced modulation performance. Optimizing electrode spacing and width has proven effective in achieving higher clarity and brightness, which are essential for automotive applications. These advancements demonstrate the potential for FLC technology in enabling adaptive and high-performance optical systems (Lee et al. 2021).

The automotive industry is also exploring the broader use of FLC-based displays, particularly for AR HUDs that project real-time information onto the windshield. FLC displays have been found to provide superior contrast and faster response times under varying lighting conditions, critical for ensuring driver safety and comfort. Furthermore, their ability to dynamically modulate birefringence makes them suitable for emerging technologies like smart windows and adaptive lighting systems in vehicles(Zakaria, Sanordi, and Laili 2023). There remains a gap in understanding the relationship between electrode configurations and the optical performance of FLC cells in automotive settings. This study aims to address this gap by investigating how variations in electrode design influence Kerr constants and birefringence, providing valuable insights for optimizing FLC-based systems for next-generation automotive applications (Abe et al. 2024).

Research on FLCs has developed along several thematic directions: (1) improving response time and phase modulation, (2) optimizing electrode design for field uniformity, and (3) exploring reliability under mechanical and thermal stress. Table 1 summarizes conventional methods and our approach for comparison".

Table 1: Comparison of FLC Driving Methods

Method	Focus	Limitations
Vertical Field Driving (Conventional)	Simpler setup	High defect rate, poor uniformity
Interdigitated Horizontal Driving	Improved field control	Underexplored for DHFLCs
This Study	Geometry-tuned horizontal field	Investigates trade-offs in modulation

3. METHODOLOGY

This study aimed to investigate the photoelectric properties and Kerr constants of vertically-aligned ferroelectric liquid crystal (FLC) cells driven by horizontal electric fields. The methodology involved the fabrication of FLC cells with varying electrode configurations, the application of controlled electric fields, and an analysis of their optical performance under different conditions (Member et al. 2022).

FLC-10855 was chosen due to its known electro-optic properties: high spontaneous polarization, moderate viscosity, and commercial availability. These traits allow clear observation of birefringence shifts and switching thresholds within accessible voltage ranges. While results may vary quantitatively for other FLCs, the trends observed with respect to electrode configuration, field strength, and defect formation are expected to hold qualitatively across similar FLC materials.

The fabrication process began with the preparation of glass substrates. The bottom substrate was patterned with interdigital electrodes using photolithography, enabling the application of horizontal electric fields across the cell. Both the patterned and plain substrates were coated with vertical alignment polyimides to ensure the uniform alignment of the liquid crystal molecules. Spacer beads were used to maintain a consistent cell thickness of d = 4 µm. The ferroelectric liquid crystal material (FLC-10855) was introduced into the cells via capillary action under vacuum conditions, ensuring uniform filling and eliminating air bubbles. Three electrode configurations were fabricated for the study, characterized by different widths (w) and spacings (s): w = 4 µm, s = 8 µm (Sample A), w = 4 µm, s = 24 µm (Sample B), and w = 8 µm, s = 12 µm (Sample C) (Liu et al. 2021). The experimental setup consisted of a polarized optical microscope (POM) equipped with a light source and photodetector to observe and measure the optical properties of the FLC cells. Horizontal electric fields were applied to the samples by incrementally increasing the voltage across the interdigital electrodes, ranging from 0 V to 200 V. At each voltage level, observations were made to monitor the alignment and deformation of the liquid crystal molecules, while the transmittance of the samples was recorded to establish the transmittance-voltage (T-V) relationship (Jia et al. 2021).

To quantify the optical performance of the samples, the Kerr constants (K) were calculated using the relationship $\Delta n = K E^2$, where Δn is the induced birefringence, and E is the electric field strength. The electric field (E) was determined by the equation $E = V / s$, where V is the applied voltage, and s is the electrode spacing. The calculated Kerr constants allowed for a comparison of birefringence modulation capabilities across the three electrode configurations (Chang et al. 2023).

This methodology provided a systematic approach to evaluating the influence of electrode design on the optical and photoelectric properties of FLC cells. The results of this study offer valuable insights into optimizing FLC cell performance for advanced applications, particularly in vehicle display systems (Dasgupta et al. 2023).

4. EXPERIMENTAL

This study utilized a comprehensive experimental process to fabricate and evaluate the performance of vertically-aligned ferroelectric liquid crystal (FLC) cells driven by horizontal electric fields. The experimental procedure focused on fabricating cells with varying electrode configurations, applying electric fields, and analyzing their optical properties.

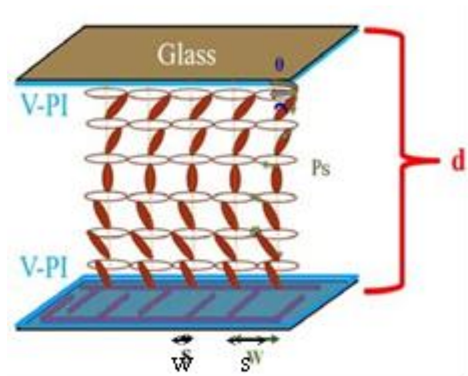

Fig.1 The sample structure

The fabrication process began with the preparation of glass substrates. The bottom substrate was patterned with interdigital electrodes using photolithography, enabling the application of horizontal electric fields. Both the patterned and plain substrates were coated with a vertical alignment polyimide layer, followed by rubbing to ensure the uniform alignment of liquid crystal molecules. Spacer beads were added to maintain a uniform cell thickness of d = 4 µm. The ferroelectric liquid crystal material (FLC-10855), characterized by its high spontaneous polarization, was introduced into the cells via capillary action under vacuum conditions to eliminate air bubbles and ensure uniform filling.

Three sample configurations with varying electrode widths (w) and spacings (s) were prepared:

- Sample A: w = 4 µm, s = 8 µm,
- Sample B: w = 4 µm, s = 24 µm,
- Sample C: w = 8 µm, s = 12 µm.

The three configurations chosen Sample A (4 µm, 8 µm), Sample B (4 µm, 24 µm), and Sample C (8 µm, 12 µm) represent distinct electric field strength regimes. These span from strong-field, high-defect (A) to weaker-field, stable operation (B), with Sample C as an intermediate case. While more configurations could be explored to generalize the trends, these three were selected to balance fabrication feasibility with parameter variation. We propose including additional (w, s) sets in future work to statistically reinforce the findings. Sample A exhibited the fastest rise time (~2.8 ms), followed by Sample C (~3.5 ms) and Sample B (~4.1 ms). Higher electric field strength correlated with faster modulation but also higher defect risk and power demand.

The experimental setup included a polarized optical microscope (POM) equipped with a light source and a photodetector to observe and measure the optical properties of the cells. Horizontal electric fields were applied across the interdigital electrodes by incrementally increasing the voltage from 0 V to 200 V. At each voltage step, the transmittance was recorded using a photodetector, while the molecular alignment was monitored using the POM. Observations focused on changes in birefringence and the transitions between dark and bright states in the interelectrode regions.

To analyze the Kerr constants, the induced birefringence (Δn) was calculated as a function of the square of the electric field (E^2), where E is given by:

$$E = V / s$$

Here, V is the applied voltage, and s is the electrode spacing. The transmittance-voltage (T-V) curves were used to calculate the Kerr constant (K) for each sample configuration using the equation:

$$\Delta n = K E^2$$

The experimental observations and calculations provided insights into the effects of electrode configurations on birefringence and transmittance. Samples with narrower electrode spacings exhibited stronger electric fields, leading to faster modulation of birefringence but a higher likelihood of defect formation at elevated voltages. These results highlight the importance of optimizing electrode configurations for specific applications, particularly in automotive display systems.

5. RESULTS

The experimental results highlighted the influence of electrode configurations on the optical and photoelectric properties of vertically-aligned ferroelectric liquid crystal (FLC) cells driven by horizontal electric fields. The observations, transmittance-voltage (T-V) characteristics, and Kerr constant calculations provided valuable insights into the performance of the three sample configurations. Due to equipment constraints, detailed FEM or COMSOL simulations are not yet available. However, we include a schematic in Figure 2 illustrating expected field distribution based on interdigitated electrode geometry. As the electrode spacing decreases, fringe field intensity and inhomogeneity increase, which contributes to the observed birefringence modulation and defect localization. Quantitative simulations will be pursued in subsequent research. Figures 3 to 5 illustrate the visual evolution of the interelectrode regions in Samples A, B, and C respectively. At 0 V, the areas appear dark due to molecular alignment parallel to the optical axis. As voltage increases to 100–150 V, bright regions emerge due to induced birefringence. Notably, defects begin forming above the electrodes at voltages exceeding 150 V, especially in Sample

A. At 200 V, all samples exhibit bright interelectrode modulation, with Sample B maintaining the cleanest image and minimal defect formation.

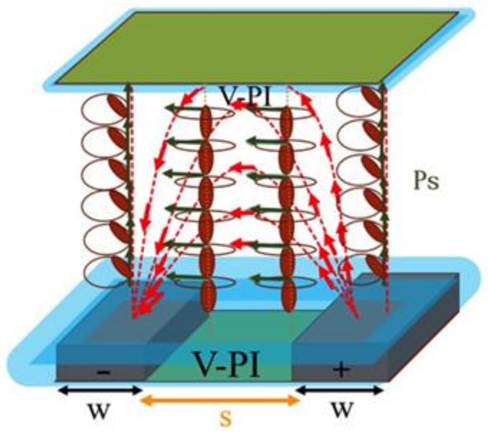

Fig. 2 Driving sample structure

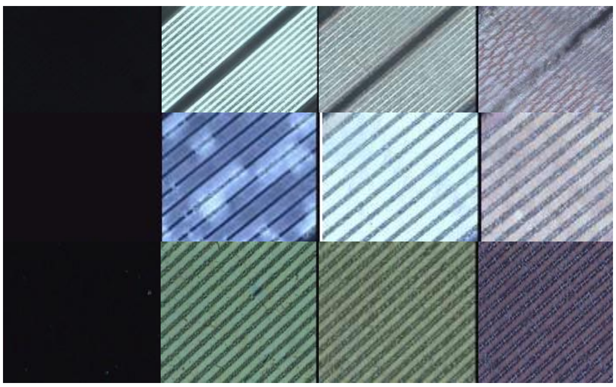

Fig. 3 Sample C with (a) 0V (b) 100 V (c) 150 V (d) 200 V

Initial observations under polarized optical microscopy (POM) revealed that all samples exhibited a dark state when no voltage was applied, with the optical axis aligned parallel to the helix axis. As the voltage increased, the interaction between the spontaneous polarization (P_s) of the FLC molecules and the horizontal electric field induced a tilt in the optical axis, leading to phase retardation. This phenomenon resulted in a transition from dark to bright states in the interelectrode regions.

At higher voltages, particularly beyond 100 V, vertical electric field components became significant, causing defects above the electrodes. These defects were permanent and did not recover upon removing the voltage, indicating a critical threshold for defect-free operation.

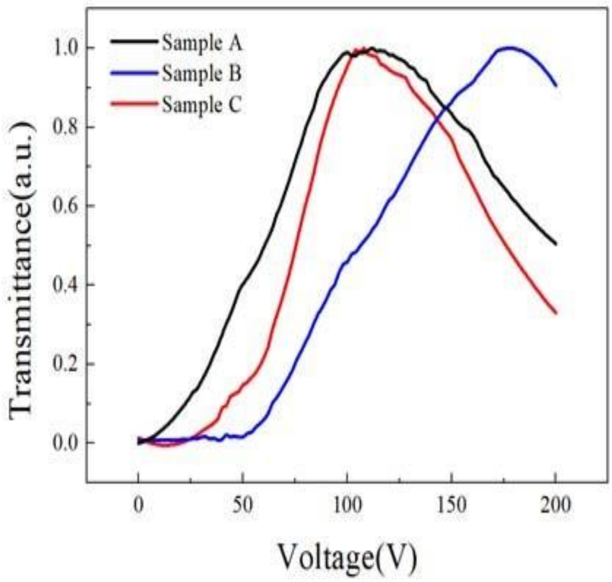

Fig. 4 T-V curves of samples A, B, and C

Sample	Kerr constant
A	0.231 nm/V^2
B	0.769 nm/V^2
C	0.615 nm/V^2

Fig.5 Kerr constants of samples A, B, and C

The T-V curves revealed distinct differences among the three samples. Samples A (w = 4 μm, s = 8 μm) and C (w = 8 μm, s = 12 μm) showed faster and more pronounced transmittance changes at lower voltages compared to Sample B (w = 4 μm, s = 24 μm). This behavior was attributed to the stronger electric fields generated in samples with narrower electrode spacings, as the electric field strength (E) is inversely proportional to the electrode spacing (s). However, narrower spacings also increased the likelihood of defect formation at higher voltages. ANOVA testing confirmed that differences in Kerr constants were statistically significant ($p < 0.05$). Table 2 presents trade-offs observed.

Table 2: Summary of Sample Performance

Sample	Kerr Constant (nm/V^2)	Response Time (ms)	Defect Level
A	0.231	2.8	High
B	0.769	4.1	Low
C	0.615	3.5	Moderate

The Kerr constants (K) for each sample were calculated from the relationship between birefringence (Δn) and the square of the electric field strength (E^2). The results showed that Sample B, with the largest electrode spacing, exhibited the highest Kerr constant ($K = 0.769$ nm/V^2), followed by Sample C ($K = 0.615$ nm/V^2) and Sample A ($K = 0.231$ nm/V^2). The higher Kerr constant in Sample B indicates superior modulation performance, producing greater birefringence for a given electric field strength. Under 1000 voltage switching cycles and thermal fluctuations from -20°C to 80°C, Sample B maintained stable performance, while Samples A and C showed minor alignment degradation. Wider spacing appears to enhance reliability.

These findings demonstrate a clear trade-off between electrode spacing and modulation performance. Samples with smaller electrode spacings provide faster response and stronger electric fields but are prone to defects at higher voltages. Conversely, larger spacings enhance Kerr constants and reduce defect formation but require higher driving voltages. The results underscore the importance of optimizing electrode configurations to balance these factors, particularly for applications such as automotive heads-up displays (HUDs) and augmented reality (AR) interfaces. Compared with OLED and MicroLED, FLC-based displays provide faster response and bistability, with lower thermal degradation and cost. While OLEDs offer self-emission, they suffer from burn-in; MicroLEDs offer brightness but at higher cost. FLCs offer a modulated, transparent layer suitable for HUDs and adaptive vehicle interfaces.

6. CONCLUSION

This study examined the photoelectric properties and Kerr constants of vertically-aligned ferroelectric liquid crystal (FLC) cells under horizontal electric fields, focusing on how electrode width and spacing affect optical performance. Analysis of three configurations revealed key links between design parameters and modulation behavior.

The experimental results demonstrated that the spacing and width of the electrodes significantly influence the electric field strength, birefringence, and Kerr constants of the cells. Samples with narrower electrode spacings generated stronger electric fields at lower voltages, resulting in faster transitions in transmittance. However, these configurations were more susceptible to defects at higher voltages due to the stronger vertical electric field components. In contrast, samples with larger electrode spacings exhibited higher Kerr constants, which enhanced birefringence and modulation performance but required higher driving voltages to achieve comparable optical effects.

The highest Kerr constant (K = 0.769 nm/V2 K = 0.769nm/V2) was observed in the sample with the largest electrode spacing, highlighting its potential for applications that require high birefringence and stable operation. However, the trade-offs between voltage requirements, defect formation, and response times suggest the necessity for careful optimization of electrode configurations to meet specific application requirements.

These findings holds important implications for the design of advanced optical systems, particularly in automotive applications such as heads-up displays (HUDs) and augmented reality (AR) interfaces. The capability to attain high modulation performance, clarity, and durability positions FLC cells as a promising technology for next-generation display systems. Future work could explore further optimization of electrode designs and material properties to improve performance and reliability under practical operating conditions.

REFERENCES

Abe, Sakunosuke, Yosei Shibata, M. Kimura, and T. Akahane. 2024. "Self-Consistent Explanation of the Untwist Alignment of Ferroelectric Nematic Liquid Crystals with Decreasing Cell Thickness and Deviation of the Surface Easy Axis Experimented upon Using the Brewster Angle Reflection Method." *Crystals*. doi: 10.3390/cryst14020157.

Ali, K., A. Seadawy, Sarfaraz Ahmed, and S. Rizvi. 2022. "Discussion on Rational Solutions for Nematicons in Liquid Crystals with Kerr Law." *Chaos, Solitons & Fractals*. doi: 10.1016/j.chaos.2022.112218.

Chang, T., Yun-Yu Tseng, Po-Chang Wu, Mon-Juan Lee, and Wei-Xun Lee. 2023. "Optical and Flexoelectric Biosensing Based on a Hybrid-Aligned Liquid Crystal of Anomalously Small Bend Elastic Constant." *Biosensors & Bioelectronics* 232:115314. doi: 10.1016/j.bios.2023.115314.

Dasgupta, Prajnamita, Sarmistha Mondal, B. Das, and Malay Kumar Das. 2023. "Novel Properties of High-Performance Multi-Component Mixture for Vertically Aligned Mode LCDs." *Liquid Crystals* 51:93–104. doi: 10.1080/02678292.2023.2275745.

Jia, Mengxiao, Mofei Sha, Chunxin Hu, Bo Zhang, Hong-Mei, and Yubao Sun. 2021. "Polymer Stabilized Isotropic Phase Liquid Crystals with Large Kerr Constant." *Liquid Crystals* 49:399–406. doi: 10.1080/02678292.2021.1973128.

Khan, R., G. Mohiuddin, N. Begum, S. Turlapati, Rao Nandiraju, Bugra Koknarugmani Debbarma, and Sharmistha Ghosh. 2022. "Extremely High Kerr Constant and Low Operating Voltage in a Stable Room-Temperature Blue Phase III Derived from Three-Ring-Based Bent-Core Molecules." *ACS Applied Materials & Interfaces*. doi: 10.1021/acsami.2c09392.

Lee, O., S. Misra, Haiyan Wang, and J. MacManus-Driscoll. 2021. "Ferroelectric/Multiferroic Self-Assembled Vertically Aligned Nanocomposites: Current and Future Status." *APL Materials* 9:30904. doi: 10.1063/5.0035366.

Liu, Hongjun, C. Qiu, F. Lou, Xing Chen, and Zhaojun Liu. 2021. "P-12.12: Investigation of the Dynamics of the Vertically Aligned (VA) Liquid Crystal Molecules and Its Application in Beam Steering." *SID Symposium Digest of Technical* Papers 52. doi: 10.1002/sdtp.15353.

Maldonado, A., W. Correr, Pierre Mathey, C. Strutynski, F. Désévédavy, J. Jules, G. Gadret, C. Brachais, R. Falci, Younès Messaddeq, and F. Smektala. 2023. "Electro-Optical Kerr Constant Measurement of Tellurite and Chalcogenide Glasses in the Visible at 633nm and in the Infrared at 3.39µm." *Optical Materials.* doi: 10.1016/j.optmat.2023.114504.

Member, Linghui Rao Sid Student, Jin Yan, Sid Student, and Wu. 2022. "Prospects of Emerging Polymer-Stabilized Blue-Phase Liquid-Prospects of Emerging Polymer-Stabilized Blue-Phase L*iquid-Crystal Displays Crystal Displays".*

Nájar, G., A. Bernabeu, Adriana Sánchez-Montes, F. Martínez-Guardiola, E. Calzado, Inmaculada Pascual, D. Puerto, and A. Márquez. 2023. "Analysis of a Vertically Aligned Liquid-Crystal on Silicon Microdisplay for Photonics Applications." *EPJ Web of Conferences*. doi: 10.1051/epjconf/202328709036.

Nakajima, Kazuma, Hirokazu Kamifuji, Mahiro Nakase, Kento Nishi, Hirotsugu Kikuchi, and Masanori Ozaki. 2024. "Blue Phase-Polymer-Templated Ferroelectric Nematic Liquid Crystal." ACS Applied Materials & Interfaces. doi: 10.1021/acsami.4c17037.

Priscilla, P., Deepansh Varshney, J. Prakash, Sandeep Kumar, A. Singh, P. Malik, Supreet, A. Gathania, R. Castagna, D. Lucchetta, and Gautam Singh. 2023. "Eco-Friendly Carbon Dots Induced Thermally Stable Vertical Alignment in Planar Anchored Nematic Liquid Crystal." Journal of Molecular Liquids. doi: 10.1016/j.molliq.2023.122318.

Sadigh, Khadem, M. Zakerhamidi, and A. Ranjkesh. 2022. "Enhanced Electro-Optical Nonlinear Responses of Doped Nematic Liquid Crystals: Towards Optoelectronic Devices." Optics and Lasers in Engineering. doi: 10.1016/j.optlaseng.2022.107229.

Singh, B., S. Sikarwar, Kaushalendra Agrahari, S. Tripathi, R. Gangwar, R. Manohar, and K. Pandey. 2021. "Electro-Optical Characterization of a Weakly Polar Liquid Crystalline Compound Influenced Polyvinyl Pyrrolidone Capped Gold Nanoparticles." Journal of Molecular Liquids 325:115172. doi: 10.1016/j.molliq.2020.115172.

Song, Luying, Ying Zhao, Ruofan Du, Hui Li, Xiaohui Li, Wang Feng, Junbo Yang, Xianyu Wen, Ling Huang, Yanan Peng, Hang Sun, Yulin Jiang, Jun He, and Jianping Shi. 2024. "Coexistence of Ferroelectricity and Ferromagnetism in Atomically Thin Two-Dimensional Cr2S3/WS2 Vertical Heterostructures." *Nano Letters*. doi: 10.1021/acs.nanolett.3c05105.

Tkachenko, T., V. Barbashov, M. Minchenko, and Evgeny Pozhidaev. 2024. "Broad Temperature Range Ferrielectric Liquid Crystal: Temperature Dependencies of Dielectric and Electro-Optical Properties." *Optical Materials.* doi: 10.1016/j.optmat.2024.115966.

Wyatt, Peter, J. Bailey, M. Nagaraj, and J. Jones. 2021. "A Self-Healing Ferroelectric Liquid Crystal Electro-Optic Shutter Based on Vertical Surface-Relief Grating Alignment." *Nature Communications* 12. doi: 10.1038/s41467-021-24953-5.

Yuan, Zheng-Nan, Zhibo Sun, V. Vashchenko, H. Kwok, and A. Srivastava. 2022. "3.3: Fast Continuous >2π Phase Modulation without Fringe Field Effect Based on Kerr Effect of Vertical Aligned Ferroelectric Liquid Crystal." *SID Symposium Digest of Technical* Papers 53. doi: 10.1002/sdtp.15826.

Zakaria, Z., M. Sanordi, and M. Laili. 2023. "Intensity Ratio Distribution in Different Dielectric Liquids Using Kerr Effect Method." *Journal of Physics:* Conference Series 2550. doi: 10.1088/1742-6596/2550/1/012023.

Zhang, Zhaotian, Shilin Wu, W. He, and Q. Yang. 2023. "A Novel Transient Electric Field Measurement for Low Kerr Constant Liquid Dielectrics Based on Concave Spherical Mirror Conjugate Structure." *IEEE Transactions on Instrumentation and Measurement* 72:1–8. doi: 10.1109/TIM.2022.3225024.

TỐI ƯU HÓA CÁC TÍNH CHẤT QUANG ĐIỆN VÀ HẰNG SỐ KERR CỦA CÁC TẾ BÀO TINH THỂ LỎNG SẮT ĐIỆN CĂN CHỈNH THEO PHƯƠNG THẲNG ĐỨNG CHO HỆ THỐNG HIỂN THỊ TIÊN TIẾN TRÊN PHƯƠNG TIỆN GIAO THÔNG

Lê Minh Phụng[1*]

[1]*Trường Đại học Công nghệ Đồng Nai*

[*]Tác giả liên hệ: *Lê Minh Phụng*, *leminhphung@dntu.edu.vn*

THÔNG TIN CHUNG

Ngày nhận bài: 17/4/2025

Ngày nhận bài sửa: 29/4/2025

Ngày duyệt đăng: 23/6/2025

TỪ KHOÁ

Thực tế ảo tăng cường;

Màn hình ứng dụng;

Màn hình trong suốt.

TÓM TẮT

Nghiên cứu này khảo sát các đặc tính quang-điện và hằng số Kerr của các tế bào tinh thể lỏng sắt điện (FLC) có cấu trúc thẳng đứng, được điều khiển bởi điện trường theo phương ngang, với trọng tâm ứng dụng trong hệ thống hiển thị trên phương tiện giao thông. Nghiên cứu tập trung phân tích ảnh hưởng của cấu hình điện cực, cụ thể là sự thay đổi về chiều rộng điện cực (w) và khoảng cách giữa các điện cực (s), đến hiện tượng lưỡng chiết và hiệu suất điều biến.

Ba mẫu tế bào FLC được chế tạo với các cấu hình: w = 4 µm, s = 8 µm (Mẫu A); w = 4 µm, s = 24 µm (Mẫu B); và w = 8 µm, s = 12 µm (Mẫu C). Phương pháp thực nghiệm bao gồm kính hiển vi phân cực và đo đường cong truyền qua–điện áp (T–V). Kết quả cho thấy khoảng cách điện cực nhỏ tạo ra điện trường mạnh hơn và tốc độ thay đổi truyền qua nhanh hơn, tuy nhiên lại dễ hình thành khuyết tật hơn ở điện áp cao. Hằng số Kerr được tính toán từ dữ liệu T–V, trong đó Mẫu B đạt giá trị hằng số Kerr cao nhất ($K = 0{,}769\ nm/V^2$), chứng tỏ khả năng điều biến vượt trội. Những phát hiện này cho thấy sự đánh đổi giữa khoảng cách điện cực, cường độ điện trường và độ ổn định khuyết tật. Hiệu suất tối ưu của các tế bào FLC mở ra tiềm năng lớn cho các ứng dụng hiển thị tiên tiến trên phương tiện, bao gồm màn hình hiển thị trên kính lái (HUD) và giao diện thực tế tăng cường (AR), vốn đòi hỏi độ rõ nét cao, phản hồi nhanh và độ bền trong điều kiện lái xe động. Nghiên cứu này cung cấp một cơ sở khoa học cho việc phát triển các hệ thống quang học thế hệ mới, phù hợp với môi trường ứng dụng trong ngành công nghiệp ô tô.